Supplementary Information

Enhancement in optically induced ultrafast THz response of $MoSe_2MoS_2$ heterobilayer

SUNIL KUMAR,[1,*] ARVIND SINGH,[1] SANDEEP KUMAR,[1] ANAND NIVEDAN,[1] MARC TONDUSSON,[2] JÉRÔME DEGERT,[2] JEAN OBERLÉ,[2] SEOK JOON YUN,[3] YOUNG HEE LEE,[3] AND ERIC FREYSZ[2,*]

[1]*Femtosecond Spectroscopy and Nonlinear Photonics Laboratory, Department of Physics, Indian Institute of Technology Delhi, New Delhi 110016, India*

[2]*Univ. Bordeaux, CNRS, LOMA UMR 5798, 33405 Talence, France*

[3]*Center for Integrated Nanostructure Physics (CINAP), Institute for Basic Science (IBS), Sungkyunkwan University, Suwon 16419, Republic of Korea*

[*]*eric.freysz@u-bordeaux.fr; kumarsunil@physics.iitd.ac.in*

1. UV-Visible absorption spectra of the TMD samples

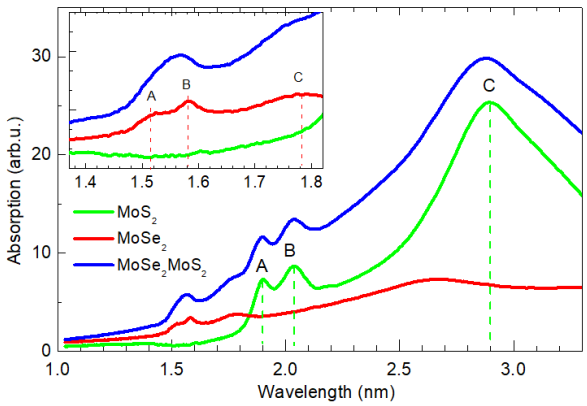

Fig. S1. UV-Visible absorption spectra of the MoS_2, $MoSe_2$ monolayers and the $MoSe_2MoS_2$ heterobilayer, all supported on quartz substrates. The main excitonic features displaying the direct band gap nature of the MoS_2 and $MoSe_2$ monolayers are marked by vertical dashed lines. There is no apparent shift in the excitonic peaks of MoS_2 or the $MoSe_2$ monolayers due to the presence of the other layer in the heterostructure. The A-, B- and C-excitonic absorption peaks in the $MoSe_2$ appear at 1.51, 1.58 and 1.79 eV, while those in MoS_2 appear at 1.90, 2.04 and 2.89 eV.

2. Raman microscopy of the $MoSe_2MoS_2$-heterobilayer

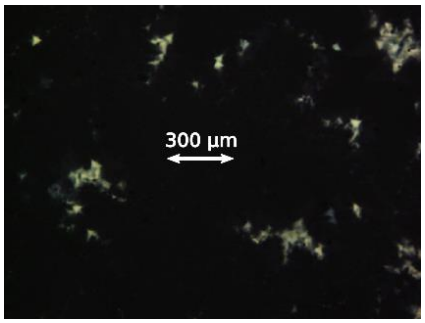

Fig. S2. Optical image of the $MoSe_2MoS_2$ heterobilayer we scanned recording Raman spectra along x and y direction using 200 µm steps. The black regions correspond to the desired material of the film while the white regions are undesired ones and represent either discontinuities or the MoS_2 monolayers on the substrate. Unambiguously, the desired material covers almost 90% of the surface of the sample. We may note that in the $MoSe_2MoS_2$-heterobilayer fabrication process, $MoSe_2$ monolayer was transferred on top of the CVD grown MoS_2 monolayer sample on the quartz substrate.

3. THz parameters of the quartz substrate from time-domain spectroscopy

THz electric field waveforms, $E_{THz}(t)$ in air and transmitted through the quartz substrate are shown in Fig. S3(a), while the corresponding spectra, $E_{THz}(\Omega)$ are presented in Fig. S3(b). It can be seen that the substrate absorbs strongly at frequencies beyond ~6 THz. The average THz absorption of the quartz substrate and the three samples, i.e., $MoSe_2$ monolayer, MoS_2 monolayer and the $MoSe_2MoS_2$-heterobilayer, can be extracted from the corresponding transmission coefficients provided in Table S1, which were obtained by analyzing the time-domain waveforms given in Fig. 1(c).

TABLE S1: THz electric field transmission coefficients (T) obtained from the maximum values of the time-domain THz electric field waveforms. The error bars are indicative of the uncertainty in the thicknesses of the quartz plates.

S.No.	Sample	Transmission coefficient $T = E_{sample}(t)/E_{air}(t)$
1	Quartz substrate	2.64/5.04 = 0.524±0.003
2	$MoSe_2$	(2.274/5.04)/0.524 = 0.861±0.004
3	MoS_2	(2.306/5.04)/0.524 = 0.873±0.004
4	$MoSe_2MoS_2$	(2.317/5.04)/0.524 = 0.877±0.004

Complex refractive index of the substrate, $n_{sub}(\Omega) = n(\Omega) + i\kappa(\Omega)$, n being the index of refraction and κ the extinction coefficient, is estimated from the following relation [1],

$$T_{sub}(\Omega) = \frac{4n_{sub}(\Omega)}{(1+n_{sub}(\Omega))^2} e^{-i\Omega d_{sub}\frac{n_{sub}(\Omega)-1}{c}} \quad \text{(S.1)}$$

In the above equation, $T_{sub}(\Omega) = E_{sub}(\Omega)/E_{air}(\Omega)$ is the experimental transmission coefficient, d_{sub} is the thickness of the substrate measured independently, c is speed of light in vacuum and Ω is angular frequency. By comparing the experimental T(Ω) with the expression in Eq. (S.1), we have extracted $n_{sub}(\Omega)$ and hence its real and imaginary parts as shown in Fig. S3(c).

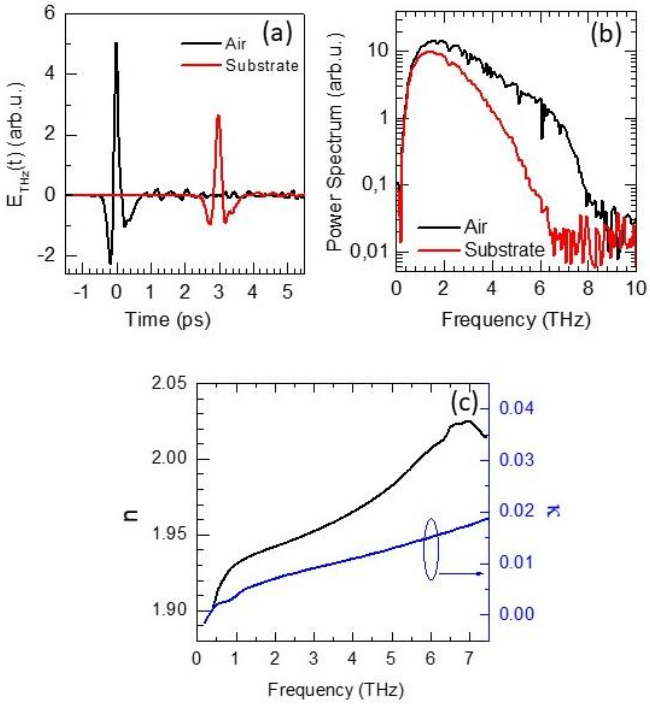

Fig. S3. THz characterization of the quartz plate used as substrate for the TMD layers studied in the paper. (a) Time-domain THz waveforms of the associated complex electric field $E_{THz}(t)$ as recorded without any sample (Air) and with the substrate. (b) Power spectra of the THz signal in air and with the substrate. The allowed THz bandwidth in the experiments is >8 THz, however, due to strong THz absorption in the substrate at frequencies beyond 6 THz, the relevant frequency range is limited to 0.2-5.5 THz. (c) Index of refraction *n* and the extinction coefficient κ of the quartz substrate extracted from the complex transmission spectra.

Our experiments performed on another quartz plate from a different batch of the substrates shows slightly different results as shown below in Fig. S4. The seemingly different THz characteristics in the two cases are not surprising because the quartz plates may vary from one batch to another, in their optical properties, more at THz frequencies at which the manufactures do not pay much attention. The results shown in the figure below match well with some of the data available in literature [2]. Of course, FTIR experiments can provide the absorption coefficients at higher frequencies but the THz time-domain spectroscopy provides the simultaneous measurement of the index of refraction also. The quartz plates used as substrates for our thin samples, were all taken from the same batch of substrates and their THz characteristics are same as shown in Fig. S3. It may be noted that this difference in the quartz substrate characteristics has no impact on the measurements and analysis of the properties of thin samples as discussed in our main paper.

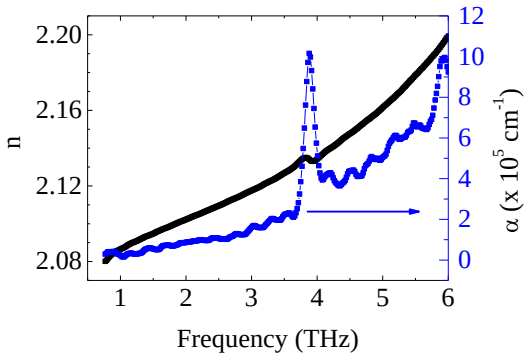

Fig. S4. The index of refraction and the absorption coefficient of a quartz plate taken from a different batch of the substrates. The parameters have been extracted using the same method as describe above in Fig. S3. These results are similar to those reported in the literature [2].

4. Data fitting procedure for the optically induced THz response

The temporal evolution of the optical pump induced THz response, i.e., the ΔR and ΔT was analyzed by numerically fitting the experimental data using a convolution function. The latter is described by the following equation,

$$Y(t) = \left(H(t)\sum_i A_i e^{-t/\tau_i}\right) \otimes \exp(-t^2/\tau_p^2) \qquad \text{(S.2)}$$

The first function H(t) on the right side of above equation is the standard Heaviside step function to account for material response at only positive times from the instant optical pump excites the sample. The temporal evolution of the material response is captured mainly by the second function, which is a sum of exponentially decaying functions having respective amplitude A_i and time-constant, τ_i. Finally, convolution of the product of the above two functions is taken with the Gaussian probe pulse having time-duration, τ_p = 200 fs as described in Eq. (S.2) to numerically fit the experimental data in our study using MATLAB.

The fitting procedure to extract the kinetic parameters (amplitudes and time-constants) of the optical pump-induced THz reflectivity and transmittance are described in Figs. S3, S4 and S5.

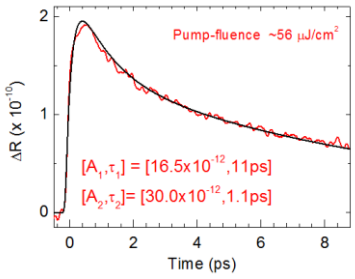

Fig. S5: Transient THz reflectivity (ΔR) of $MoSe_2MoS_2$ heterostructure recorded for optical pump wavelength (photon energy) of 400 nm (3.1 eV) shown here to demonstrate the data fitting procedure at a given optical pump-fluence as mentioned. Convolution of a tri-exponentially decaying function with a

Gaussian probe pulse having FWHM of 200 fs is used to fit the data. The fit is shown using thick black curve. The major components are [A_1,τ_1; A_2,τ_2]: A's are the amplitudes and τ's are corresponding decay time constants while the slowest component [A_3,τ_3] with decay time-constant > 100 ps is negligibly small.

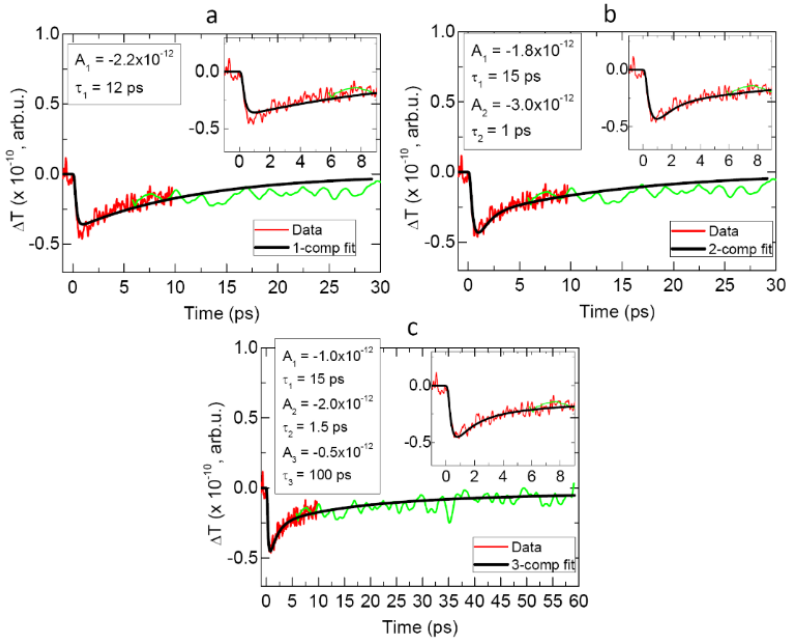

Fig. S6. Comparison between data fitting using one-, two- and three-component exponentially decaying function convolved with the Gaussian probe pulse. The data shown here is for the transient THz transmission change ΔT in $MoSe_2$ at optical pump wavelength (photon energy) of 800 nm (1.5 eV) and pump-fluence of ~215 $\mu J/cm^2$. The signals obtained are extremely weak at this pump wavelength. Data with the fits are shown using (a) one-component, (b) two-component, and (c) three-component decaying function in a large time-window. The insets show the same data in narrow time window around the zero delay. Fits in each case have been shown using thick black curves and the corresponding fit parameters have also been mentioned therein. A's are the amplitudes and τ's are the corresponding decay time constants. Clearly, the best fit is obtained for a three-component decaying function having the slowest components being significantly small in comparison with the first two.

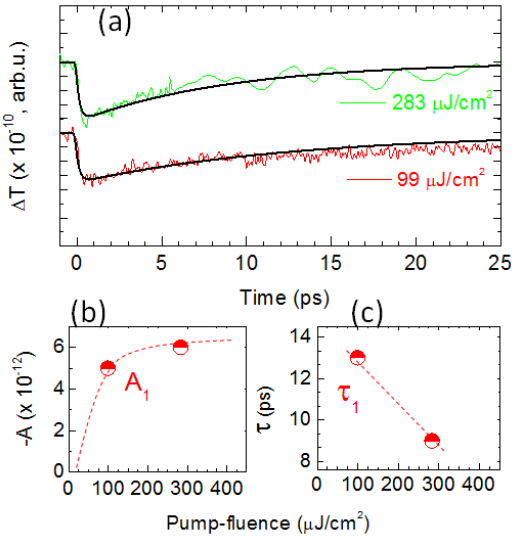

Fig. S7. Optical pump at 800 nm (photon energy 1.5 eV) induced changes in the transient THz probe transmittance signal (ΔT) recorded on $MoSe_2MoS_2$ heterostructure at medium and high pump-fluences as mentioned. The signals are quite weak even under the optimized experimental conditions. The data in (a) can be fitted reasonably well with just single exponentially decaying function having its amplitude A_1 and

time-constant τ_1 varying with the fluence as shown in the lower panels (b) and (c), respectively. A very weak third component (not shown here) with its time-constant (>100 ps) is required to ensure the best fitting of the data at longer times. We may note that even at such high pump-fluences, the signature of the fast decay constant (~1ps) is absent.

5. Optical pump-THz probe experiments performed on MoS_2 monolayer at 1.55 eV optical excitation

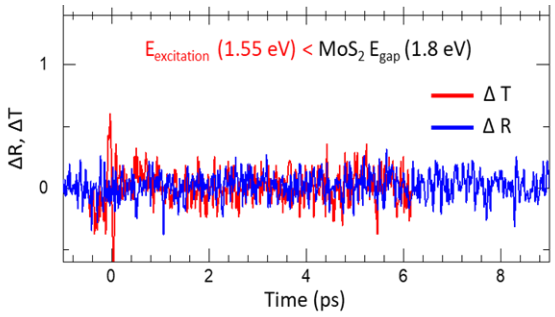

Fig. S8. Optical pump at 800 nm (photon energy 1.5 eV) induced changes in the transient THz probe transmittance (ΔT) and reflectance (ΔR) signals recorded on MoS_2 monolayer at high pump-fluence of ~400 μJ/cm^2.

6. THz conductivity from the pump-induced change in THz response

One can roughly estimate the change in the THz conductivity [3] using the following expression valid at normal incidence,

$$\Delta\sigma(\Omega) = \frac{n_s^2-1}{2Z_0}\frac{\Delta E(\Omega)}{E(\Omega)} \quad \text{(S.3)}$$

Here, n_s and Z_0 are the index of the substrate and the impedance of vacuum, respectively. Accordingly, for MoS_2MoSe_2 heterostructure at 800 nm, for a fluence of 382 μJ/cm^2, we find the change in amplitude is ~1.8%, which corresponds to a change in the sheet conductivity of ~0.01 mS.

7. Sample uniformity

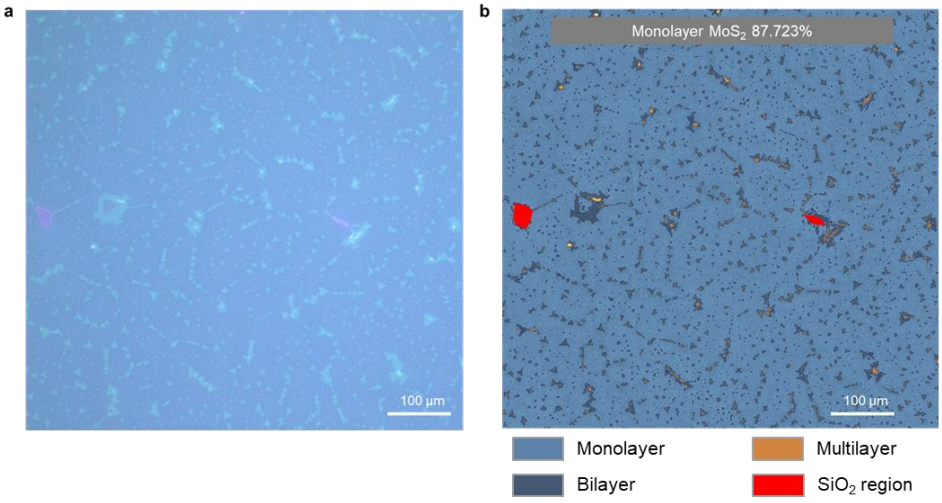

Fig. S9. a. Optical image of CVD-grown MoS_2 film sample. b. Monolayer-area marked image by free software of Gwyddion.

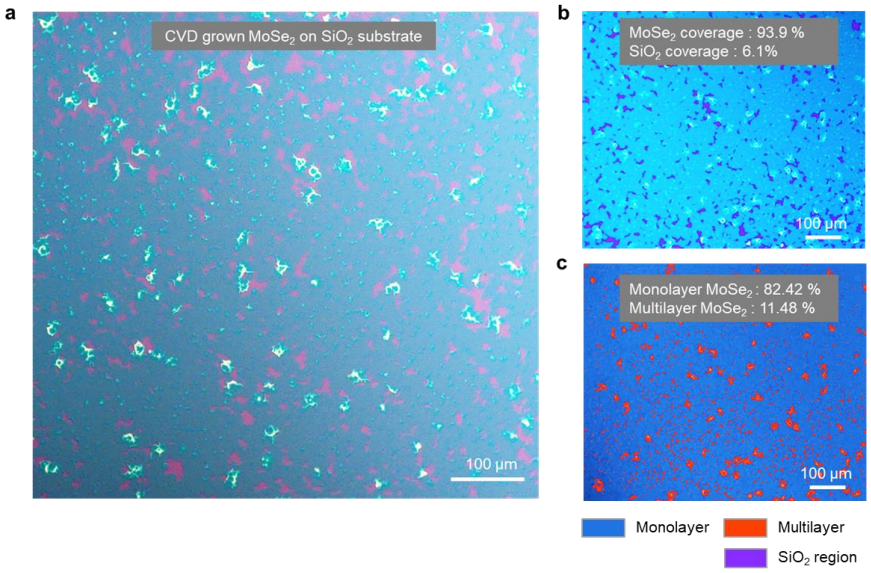

Fig. S10. a. Optical image of CVD-grown $MoSe_2$ sample. $MoSe_2$-area (b) and monolayer $MoSe_2$ (c) marked image by free software of Gwyddion.

References:

1. H. J. Joyce, J. L. Boland, C. L. Davies, S. A. Baig and M. B. Johnston, A review of the electrical properties of semiconductor nanowires: insights gained from terahertz conductivity spectroscopy, Semicond. Sci. Technol. 31, 103003 (2016).
2. C. L. Davies, J. B. Patel, C. Q. Xia, L. M. Herz and M. B. Johnston, Temperature-Dependent Refractive Index of Quartz at Terahertz Frequencies, Journal of Infrared, Millimeter, and Terahertz Waves 39, 1236–1248 (2018).
3. F. D'Angelo, Ultra-Broadband Terahertz Spectroscopy with Terahertz Air Photonics, PhD thesis (2016), Faculty of Science (FNWI), University of Amsterdam.